

First passage time densities in resonate-and-fire models

T. Verechtchaguina, I. M. Sokolov, and L. Schimansky-Geier

Institute for Physics, Humboldt-University at Berlin, Newton Strasse 15, D-12489 Berlin, Germany

(Received 17 November 2005; published 13 March 2006)

Motivated by the dynamics of resonant neurons we discuss the properties of the first passage time (FPT) densities for non-Markovian differentiable random processes. We start from an exact expression for the FPT density in terms of an infinite series of integrals over joint densities of level crossings, and consider different approximations based on truncation or on approximate summation of this series. Thus the first few terms of the series give good approximations for the FPT density on short times. For rapidly decaying correlations the decoupling approximations perform well in the whole time domain. As an example we consider resonate-and-fire neurons representing stochastic underdamped or moderately damped harmonic oscillators driven by white Gaussian or by Ornstein-Uhlenbeck noise. We show that approximations reproduce all qualitatively different structures of the FPT densities: from monomodal to multimodal densities with decaying peaks. The approximations work for the systems of whatever dimension and are especially effective for the processes with narrow spectral density, exactly when Markovian approximations fail.

DOI: [10.1103/PhysRevE.73.031108](https://doi.org/10.1103/PhysRevE.73.031108)

PACS number(s): 05.40.-a, 02.50.Ey, 87.17.Nn

I. INTRODUCTION

The first passage time (FPT) is the time T when a stochastic process $x(t)$ leaves an *a priori* prescribed domain Δ of its state space for the first time, assumed that $x(t)$ has been started at $t=0$ from a given initial value within Δ . This concept was originally introduced by Schrödinger when discussing behavior of Brownian particles in external fields [1]. A large variety of problems ranging from noise in vacuum tubes, chemical reactions, and nucleation [2] to stochastic resonance [3], behavior of neurons [4], and risk management in finance [5] can be reduced to FPT problems. In the majority of applications the attractor of the system's dynamics lies inside Δ . The escape process is characterized by the noise-induced flux through the absorbing boundary of Δ , i.e., by the probability density $\mathcal{F}(T)$ of the first passage time.

Approaches to find $\mathcal{F}(T)$ are typically based either on the Fokker-Planck equation with an absorbing boundary [6] or on the renewal theory [7]. Despite the long history, explicit expressions for the FPT density are known only for a few cases. These include overdamped particles under the influence of white noise in the force-free case, under time-independent constant forces and linear forces [4,8–10], as well as the case of a constant force under colored noise [11]. Reasonable approximations exist for a few nonlinear forces [12,13]. The FPT densities of stationary Markovian processes have a very habitual form: $\mathcal{F}(T)$ goes through a single maximum and then it decays either exponentially or as a power law. Many neuronal systems do demonstrate such kind of behavior. It was shown already in Ref. [9] that the interspike interval (ISI) histograms obtained experimentally from output of some neurons can be reproduced by FPT densities of the one-dimensional diffusion process.

This kind of description is suitable for overdamped systems, where the relaxation time to the attractor t_{rel} is much smaller than the typical first passage time. At first the local *quasiequilibrium* is established in the system. The escape occurs then from this equilibrium state and follows with a

constant rate κ inversely proportional to the mean FPT. This situation is closely related to Kramer's problem considering the quasistationary flux over transparent boundary in the low noise limit. The problem is independent of the detailed initial state and of the time the trajectory has spent inside Δ . At times T exceeding t_{rel} the FPT probability density decays exponentially: $\mathcal{F}(T) \sim \exp(-\kappa T)$. Well-known examples are chemical systems and nucleation processes, where the rates determine the mean velocity of chemical reactions or of forming overcritical nuclei [2]. Other examples are the leaky integrate-and-fire and similar neuronal models, where after the reset the corresponding trajectories approach quickly the stable rest state [14].

However, if the time scale separation between the relaxation and escape does not hold, the escape can occur before the establishment of the quasiequilibrium and the rates are time dependent. The first passage time depends sensitively on the initial conditions and the FPT densities have a complex shape different from an exponential decay. This is the case in the presence of metastable states [15,16]. Another example is pertinent to short time scales $T < t_{rel}$, which attracted growing interest because of recent experiments studying chemical reactions on time scales down to femtoseconds. The flux over the boundary before the establishment of the quasiequilibrium was found to grow in a stepwise manner, for an underdamped potential system staying initially at the bottom of the well [17].

Our work is mainly motivated by dynamics of resonant neurons [18–20]. The voltage variable of such a neuron exhibits damped subthreshold oscillations around the attractive rest state. The characteristic relaxation time to the rest state is large compared to the mean ISI. The escape of the voltage over the excitation threshold is the beginning of a new spike. After spiking the voltage variable is reset to a fixed value far from the rest state and then it can reach the threshold *prior* relaxation to the rest. The interspike interval densities obtained from the output of resonant neurons show a sequence of decaying peaks separated by intervals whose length is of

the order of the period of subthreshold oscillations. In contrast to Kramer's rate theory we stress again the nonstationary character of this problem due to the reset to sharp initial conditions.

The multimodal ISI probability densities can be reproduced in models with different mechanisms of subthreshold resonance: in the Hodgkin-Huxley model [21], in the excitable FitzHugh-Nagumo model with the stable fix point being a focus [22,23], or in the region of a canard bifurcation [24,25]. It was also shown that two-component approximations might well mimic the spiking activity of the stochastic Hodgkin-Huxley system [26]. All these models have in common that the multimodal FPT density is obtained for stochastic dynamical systems, which have at least two dynamical variables, exhibit weakly, moderately damped or self-amplifying oscillations, and after a spike reset to initial values which are not a fixed point. In the noise-free situation these systems were denoted resonate-and-fire neurons [27].

In the present work we aim to model excitable behavior with damped subthreshold oscillations. First we present the general exact expression for the FPT density for stochastic processes with differentiable trajectories [10,28–30]. It results in an infinite series of integrals over joint densities of multiple level crossings. The later sum stands for a sequential summing of trajectories excluding all except the ones yielding the first passage. Furthermore, we discuss approximations for FPT densities, which are based either on truncation of this series, or on its approximate summation based on decoupling. We prove the quality of different approximations by explicit calculations for an underdamped harmonic oscillator driven by white or colored Gaussian noise, representing the stochastic resonate-and-fire neurons.

II. EXACT EXPRESSION FOR THE FIRST PASSAGE TIME DENSITY

Consider a single random variable $x(t)$, whose t -dependence is assumed to be differentiable. The first passage problem for $x(t)$ to a boundary x_b is a special case of a level crossing problem.

The general theory of level crossings by a random process was originally put forward by Rice [28]. He derived an expression for the probability density of recurrence of a stationary random process to a given level in the form of the so-called Wiener-Rice series [29]. The exact expression for the first passage time probability density Eq. (7) is analogous to the Wiener-Rice series and was discussed in Ref. [30], where the main result, our Eq. (7), was proved. We proceed by giving a much more elementary derivation of Eq. (7) which serves as the main instrument in our further investigations.

Let us first discuss the probability $n_1(x_b, t | x_0, v_0) dt$ that a continuous differentiable process $x(t)$ crosses the level x_b in a time interval between t and $t+dt$ with positive velocity $v(t)=\dot{x}(t)>0$ under initial conditions $x(0)=x_0, \dot{x}(0)=v_0$. Generally the whole set of variables resulting from the Markovian embedding of $x(t)$ should be given at $t=0$. For simplicity we consider two-dimensional dynamics, generalization for the higher dimensional systems is obvious. Crossing

the level with positive velocity will be referred to as an upcrossing in what follows.

If $x(t)$ crosses the barrier within time interval $(t, t+dt)$ with velocity $v>0$, then the value of coordinate at time t should lie in interval $x_b - v dt < x(t) < x_b$. The probability that $x(t)$ is in this interval equals $\int_{x_b - v dt}^{x_b} P(x, v, t | x_0, v_0, 0) dx = |v| P(x_b, v, t | x_0, v_0, 0) dt$. Now, the velocity value at the instant of crossing is positive but otherwise arbitrary. Thus we obtain the probability density of an upcrossing by integration over all positive v :

$$n_1(x_b, t | x_0, v_0, 0) = \int_0^\infty v P(x_b, v, t | x_0, v_0, 0) dv. \quad (1)$$

Equation (1) can be simply generalized to give the expression for the joint probability density of multiple upcrossings. The probability $n_p(x_b, t_p; \dots; x_b, t_1 | x_0, v_0, 0) dt_p \dots dt_1$, that the process $x(t)$ crosses the level x_b in each of p time intervals $(t_1, t_1 + dt_1), \dots, (t_p, t_p + dt_p)$ is given by

$$\begin{aligned} n_p(x_b, t_p; \dots; x_b, t_1 | x_0, v_0, 0) \\ = \int_0^\infty dv_p \dots \int_0^\infty dv_1 v_p \dots v_1 \\ \times P(x_b, v_p, t_p; \dots; x_b, v_1, t_1 | x_0, v_0, 0). \end{aligned} \quad (2)$$

In what follows we omit x_b and initial conditions in expressions for the joint densities of upcrossings. The transition probability densities are connected with joint probability densities according to Bayes' theorem:

$$\begin{aligned} P(x_p, v_p, t_p; \dots; x_b, v_1, t_1; x_0, v_0, 0) \\ = \frac{P_{2p+2}(x_p, v_p, t_p; \dots; x_b, v_1, t_1 | x_0, v_0, 0)}{P_2(x_0, v_0, 0)}. \end{aligned} \quad (3)$$

Our aim now is to calculate the first passage time probability density $\mathcal{F}(T)$ that is the fraction of all trajectories starting from the initial point x_0 with initial velocity v_0 which perform the upcrossing of the barrier at time T and this upcrossing is the first one. All such trajectories are accounted for in probability density $n_1(T)$ (see the first row in Fig. 1). However, $n_1(T)$ also accounts for trajectories for which the upcrossing at time T was not the first one, i.e., which had another upcrossing at some earlier time $t_1 < T$ (row 2 in Fig. 1). Such trajectories should not contribute to $\mathcal{F}(T)$, therefore we should subtract them from $n_1(T)$. Taking into account that t_1 can be arbitrary between 0 and T , we get

$$n_1(T) - \int_0^T n_2(T, t_1) dt_1. \quad (4)$$

This excludes all trajectories which cross x_b exactly twice until T . However, Eq. (4) does not fully solve the problem since the trajectories crossing x_b three times, i.e., at time T and at two earlier moments $t_i < T, i=1, 2$ (row 3 in Fig. 1), are not accounted for correctly. Each such trajectory is counted once in $n_1(T)$. The second term in Eq. (4) accounts for the pairs of upcrossings at T and at some $t_i < T$. Each trajectory with two additional upcrossings at $t_i < T, i=1, 2$ is therefore subtracted twice in $\int_0^T n_2(T, t_1) dt_1$. Such trajectories

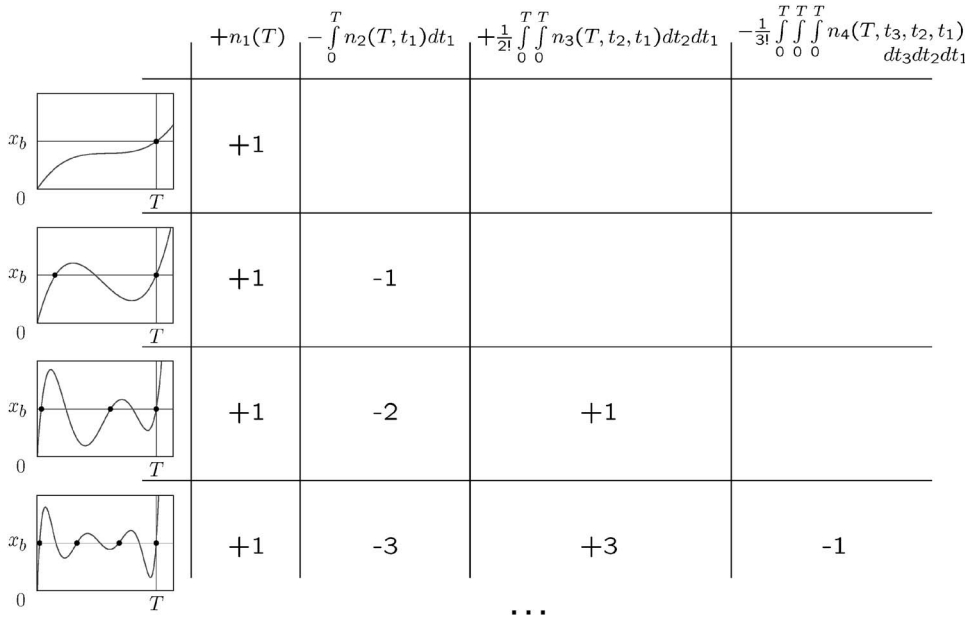


FIG. 1. Counting crossings. The N th row corresponds to trajectories with exactly N upcrossings. The p th column corresponds to the p th term of the sum Eq. (6). The number on their intersection gives how many times a trajectory with exactly N upcrossings is accounted for in the p th term. The sum of all numbers in every row is exactly zero.

should not contribute to $\mathcal{F}(T)$: in Eq. (4) we subtracted too much and have to add the amount of trajectories with three upcrossings at times $0 < t_i < T, i=1, 2$ and T again:

$$n_1(T) - \int_0^T n_2(T, t_1) dt_1 + \frac{1}{2!} \int_0^T \int_0^T n_3(T, t_2, t_1) dt_2 dt_1. \quad (5)$$

The factor $1/2!$ in the last term accounts for the number of permutations of variables t_i . Generally, if a trajectory crosses the level at time T and at N earlier times $t_i < T, i=1, \dots, N$, then in $\frac{1}{p!} \int \dots \int n_{p+1}(T, t_p, \dots, t_1) dt_1 \dots dt_p$ it is accounted for exactly C_N^p times (C_N^p stands for the number of combinations). Note that $\sum_{p=0}^N (-1)^p C_N^p = (1-1)^N = 0$. Thus in the alternating sum of the kind Eqs. (4) and (5) containing $N+1$ terms, all trajectories crossing x_b at time T and having $i=1, 2, \dots, N$ additional upcrossings are excluded, however, the ones with the larger number of upcrossings are not accounted for correctly. Extending the sum to infinity we exclude all superfluous trajectories, and only trajectories, for which the upcrossing at time T was the first one, remain. Thus the expression for the first passage time probability density reads

$$\mathcal{F}(T) = \sum_{p=0}^{\infty} \frac{(-1)^p}{p!} \int_0^T \dots \int_0^T n_{p+1}(T, t_p, \dots, t_1) dt_p \dots dt_1. \quad (6)$$

Explicitly expressing the joint densities of upcrossings using Eqs. (2) and (3), we get

$$\begin{aligned} \mathcal{F}(T) &= \frac{1}{P_2(x_0, v_0, 0)} \sum_{p=0}^{\infty} \frac{(-1)^p}{p!} \int_0^T \dots \int_0^T dt_p \dots dt_1 \\ &\times \int_0^{\infty} \dots \int_0^{\infty} dv dv_1 \dots dv_p v v_1 \dots v_p \\ &\times P_{2p+4}(x_b, v, T; x_b, v_p, t_p; \dots; x_b, v_1, t_1; x_0, v_0, 0). \end{aligned} \quad (7)$$

Equation (6) connects $\mathcal{F}(T)$, i.e., the solution of the FPT problem with absorbing boundary at x_b , with all joint densities of upcrossings for the unbounded process. To obtain $n_p(t_p, \dots, t_1)$ we consider trajectories, which are not absorbed at x_b , but can return after an upcrossing and then cross x_b again and again. The right combination of all these densities of multiple level crossings results in the probability density for the first upcrossing.

An alternative to direct summation of infinite series Eq. (6) is based on an analog to a cumulant expansion. The times when the random process $x(t)$ performs upcrossings of x_b form a *point process*, or a *system of random points* [7,10]. The functions

$$n_1(t_1), \quad n_2(t_2, t_1), \quad n_3(t_3, t_2, t_1), \dots \quad (8)$$

are the *distribution functions* of the point process. Since $x(t)$ has finite velocity, the interval between two upcrossings cannot be arbitrary small and so $n_p(t_p, \dots, t_1)$ vanishes if two of its arguments coincide. Such random point process is called a *system of nonapproaching points* [10]. In this context $\mathcal{F}(T)$ is interpreted as the waiting-time density of the point process. The last is the probability density for the time T when the first event occurs.

The system of random points is completely characterized by its cumulant functions

$$g_1(t_1), \quad g_2(t_2, t_1), \quad g_3(t_3, t_2, t_1), \dots \quad (9)$$

Choose an arbitrary natural number r , and then fix r arbitrary numbers z_1, \dots, z_r and r positive times t_1, \dots, t_r . The cumulant functions are then defined by the relation

$$\begin{aligned} 1 + \sum_{p=1}^{\infty} \frac{1}{p!} \sum_{\alpha, \dots, \omega=1}^r n_p(t_\alpha, \dots, t_\omega) z_\alpha \dots z_\omega \\ = \exp \left(\sum_{p=1}^{\infty} \frac{1}{p!} \sum_{\alpha, \dots, \omega=1}^r g_p(t_\alpha, \dots, t_\omega) z_\alpha \dots z_\omega \right). \end{aligned} \quad (10)$$

We obtain the explicit relations between cumulant and distribution functions of the point process if we differentiate both sides of Eq. (10) over all z_i and then set $z_i=0$ ($i=1, \dots, r$), i.e., if we apply the operator $\partial^r / (\partial z_1 \cdots \partial z_r) |_{z_1=\dots=z_r=0}$. Doing so sequentially for $r=1, 2, 3, \dots$ we get

$$\begin{aligned} g_1(t_1) &= n_1(t_1), \\ g_2(t_2, t_1) &= n_2(t_2, t_1) - n_1(t_1)n_1(t_2), \\ g_3(t_3, t_2, t_1) &= n_3(t_3, t_2, t_1) - 3\{n_1(t_1)n_2(t_3, t_2)\}_s \\ &\quad + 2n_1(t_1)n_1(t_2)n_1(t_3), \dots \end{aligned} \quad (11)$$

Here $\{\cdots\}_s$ denotes the operation of symmetrization of the expression in the brackets with respect to all permutations of its arguments. The coefficients in these forms are the same as in relations between the moments and the cumulants of a random variable.

The relation Eq. (10) does not change its form if we choose different times t_1, \dots, t_r , different values z_1, \dots, z_r , or change the number r . Thus extending r to infinity, allowing t to take all possible values between 0 and T , and choosing $z_1=\dots=z_r=-1$ we get from Eq. (10)

$$\begin{aligned} 1 + \sum_{p=1}^{\infty} \frac{(-1)^p}{p!} \int_0^T \cdots \int_0^T n_p(t_p, \dots, t_1) dt_p \cdots dt_1 \\ = \exp \left(\sum_{p=1}^{\infty} \frac{(-1)^p}{p!} \int_0^T \cdots \int_0^T g_p(t_p, \dots, t_1) dt_p \cdots dt_1 \right). \end{aligned} \quad (12)$$

It is easy to verify that the derivative ($-d/dT$) of the expression on the left-hand side of Eq. (12) is exactly the expression on the right-hand side of Eq. (6). Thus differentiating the right-hand side of Eq. (12) over T we obtain the expression for the waiting-time density $\mathcal{F}(T)$ through the cumulant functions of the point process:

$$\mathcal{F}(T) = S'(T)e^{-S(T)} \quad (13)$$

with

$$S(T) = - \sum_{p=1}^{\infty} \frac{(-1)^p}{p!} \int_0^T \cdots \int_0^T g_p(t_p, \dots, t_1) dt_p \cdots dt_1. \quad (14)$$

Equations (9)–(12) are general expressions which hold for systems of random points, defined by distribution functions Eq. (8) of any kind. So are also Eqs. (6), (13), and (14), which give the waiting-time density for arbitrary point process. In particular, for the random points being the times, when a differentiable random process crosses the level x_b , the distribution functions $n_p(t_p, \dots, t_1)$ are given by the joint densities of upcrossings Eq. (2). Then Eqs. (6), (13), and (14) together with Eq. (2) express the first passage time density for this differentiable random process. The function $S'(T)$ can be interpreted as the time-dependent escape rate.

These are the exact results for the FPT probability density of any continuous differentiable random process. Though these results were employed for mathematical proofs, to our knowledge these infinite series of multiple integrals was never used for explicit calculations. We proceed to show that Eqs. (6), (13), and (14) can be a starting point for several approximations. As often in the case of infinite series, the useful approximations can be based either on the truncation of the series after several first terms calculated exactly, or by approximation of the higher order terms through the lower order ones that might lead to a closed analytical form. Truncation approximations for Eq. (6) are not normalized, hold only on short time scales, and diverge at longer times (due to the miscount of trajectories with several upcrossings). The approximations of the second type are based on a subsummation in Eq. (14) for $S(T)$. They are normalized and can be used in the whole time domain. Note, only approximations guaranteeing positive rates $S'(T)$ are reasonable. Thus the set of possible approximations for the series Eq. (14) is rather restricted.

III. NOISY DRIVEN HARMONIC OSCILLATOR: RESONATE-AND-FIRE

The model we have in mind is the resonate-and-fire model of a neuron [27]. This is the least complicated model accounting for the resonant properties of neurons in terms of an equivalent RLC circuit [18,19]. In this way it is directly related to the leaky integrate-and-fire model also based on the electrical analogy. Alternatively the model can be interpreted as a systematic and linearized reduction of Hodgkin-Huxley type dynamics [31]. For the sake of simplicity we neglect the absolute refractory time. Under this assumption the model is equivalent to the underdamped harmonic oscillator with the threshold and reset, what makes the results applicable in many other domains of science. We change by time scale and variable transformations to dimensionless parameters and variables. The dynamics of the voltage variable $x(t)$ is given by

$$\dot{x} = v; \quad \dot{v} = -\gamma v - \omega_0^2 x + \eta(t). \quad (15)$$

We fix the frequency $\omega_0=1$, choose initial conditions for x and its velocity v to be $x_0=-1$, $v_0=0$, and set the threshold at $x_b=1$. In the present paper we consider two types of noisy drive: (i) the white noise $\eta(t)=\sqrt{2D}\xi(t)$, and (ii) the Ornstein-Uhlenbeck noise $\dot{\eta}=-\tau^{-1}\eta+\sqrt{2D}\tau^{-1}\xi(t)$, with $\xi(t)$ being the white Gaussian noise of intensity 1. First we concentrate on the case (i) of white noise driving.

Because of the linearity of the system Eq. (15) all joint probability densities are Gaussian and have the form [6]

$$P_n(\vec{Q}) = \frac{1}{(2\pi)^{n/2} \sqrt{\det \hat{C}_n}} \exp \left(-\frac{\vec{Q} \hat{C}_n^{-1} \vec{Q}}{2} \right). \quad (16)$$

Here $\vec{Q}=[q_1(t_1), \dots, q_n(t_n)]$ is an n -dimensional vector, whose i th component is the value of coordinate $x(t_i)$ or of velocity $v(t_i)$ at the moment t_i . \hat{C}_n is a symmetric $n \times n$ correlation matrix. Its elements are correlation functions be-

tween corresponding components of vector \vec{Q} : $c_{ij}=c_{ji}=\langle q_i(t_i)q_j(t_j) \rangle$.

Correlation functions for the system Eq. (15) are easily obtained using Fourier transform and Wiener-Khinchin theorem [6]. For the case of white noise driving and in an underdamped regime ($\gamma < 2\omega_0$) $r_{xx}(t)=\langle x(t')x(t'+t) \rangle = \frac{D}{\gamma\omega_0^2} e^{-\gamma/2t} \left[\frac{\gamma}{2\Omega} \sin(\Omega t) + \cos(\Omega t) \right]$, with $\Omega = \sqrt{|\omega_0^2 - \frac{\gamma^2}{4}|}$. In overdamped case ($\gamma > 2\omega_0$) the expression for $r_{xx}(t)$ is the same, except the trigonometric functions are replaced with hyperbolic ones. Further, $r_{xv}(t)=r'_{xx}(t)$ and $r_{vv}(t)=-r''_{xx}(t)$.

Then $n_1(T)$ is obtained from Eq. (1) in closed analytical form:

$$n_1(T) = \frac{\sigma_x \sigma_v}{2\pi \mu_{22} \sqrt{\det \hat{C}_4}} \exp \left[\frac{\sigma_x^2 v_0^2 + \sigma_v^2 x_0^2}{2\sigma_x \sigma_v} \right] \times \exp \left[-\frac{1}{2} \sum_{i,j \neq 2} \mu_{ij} q_i q_j \right] [1 - \sqrt{\pi} \alpha e^{\alpha^2} \text{erfc}(\alpha)]. \quad (17)$$

Here $\mu_{ij}=\mu_{ji}$ are elements of the inverse correlation matrix $(\hat{C}_4)^{-1}$, and q_i are components of the vector $\vec{Q}=[x(T), v(T), x_0(0), v_0(0)]$. The dispersions of x and v are $\sigma_x^2=r_{xx}(0)=D/\gamma\omega_0^2$, $\sigma_v^2=r_{vv}(0)=D/\gamma$. We have introduced $\alpha=(\sum_{i \neq 2} \mu_{2i} q_i)/\sqrt{2\mu_{22}}$. Finally, $\text{erfc}(x)$ is a complementary error function.

For the joint densities of multiple upcrossings $n_p(t_p, \dots, t_1)$ no closed expressions can be obtained. We evaluate the integral over v_1 in Eq. (2) analytically and then perform numerical integration of the resulting expression over v_2, \dots, v_p to obtain $n_p(t_p, \dots, t_1)$. The integrals over time in the expressions for $\mathcal{F}(T)$ are also evaluated numerically.

IV. TRUNCATION APPROXIMATIONS

The first passage time density $\mathcal{F}(T)$ for the harmonic oscillator driven by white Gaussian noise obtained from simulations is depicted with black crosses in Fig. 2. Parameters are chosen to be $\gamma=0.01$, $D=0.02$. In this case of very small friction the correlation functions of the process oscillate with period $T_p=2\pi/\sqrt{\omega_0^2-\gamma^2/4}$ and decay slowly within the relaxation time $t_{rel}=2/\gamma$. A typical trajectory is smooth and shows almost regular oscillations with fluctuating phase and amplitude. The probability to reach x_b is higher in the maxima of the subthreshold oscillations. The initial phase of these oscillations is fixed by sharp initial conditions. Thus on shorter time scales $\mathcal{F}(T)$ shows the multiple peaks following with the frequency of damped oscillations $\Omega=\sqrt{\omega_0^2-\gamma^2/4}$. On long times $T \gg t_{rel}$ the quasiequilibrium establishes and FPT density decays exponentially. The number of visible peaks depends on the relation between t_{rel} and the period of oscillations T_p and is given by the number of periods elapsing before the quasiequilibrium is achieved. For parameter values as in Fig. 2 $t_{rel}=200$, which corresponds to about 30 periods $T_p=6.28$.

Let us consider truncation approximations for the series Eq. (6). The first approximation is given by the first term

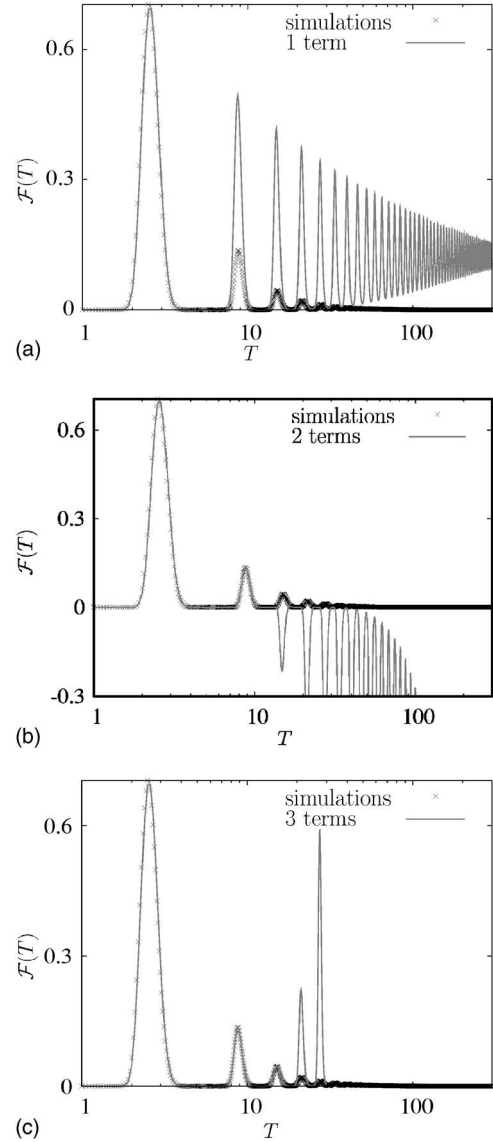


FIG. 2. FPT density for harmonic oscillator driven by white Gaussian noise, $\omega_0=1$, $\gamma=0.01$, $D=0.02$, $x_0=-1$, $v_0=0$, and $x_b=1$. Simulation results are shown with black crosses and truncation approximations with a gray line: (a) one term Eq. (1), (b) two terms Eq. (4), and (c) three terms Eq. (5). The mean FPT obtained from simulations equals 14.6, the median of distribution lies by 3.2. Note the logarithmic scale.

$n_1(T)$, the second approximation by two terms, Eq. (4), and the third by three terms, Eq. (5). The higher order approximations entail the numerical estimation of high-dimensional integrals, which at some stage leads to a computational effort larger than the one necessary for a direct simulation. Therefore we restrict ourselves to the one-, two-, and three-term approximations.

The result of the one term approximation is shown in Fig. 2(a) with a gray line. The first peak of the FPT density is reproduced almost exactly. All further peaks are overestimated because all trajectories performing multiple upcrossings of x_b are included. On long times the process becomes stationary and the first approximation tends to a constant value $\lim_{T \rightarrow \infty} n_1(T) = n_0$. This is the mean frequency of up-

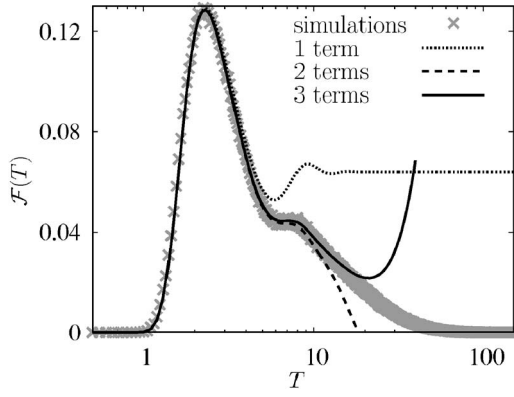


FIG. 3. FPT density for harmonic oscillator driven by white Gaussian noise, $\omega_0=1$, $\gamma=0.8$, $D=0.44$, $x_0=-1$, $v_0=0$, and $x_b=1$. Simulation results shown with gray crosses; one term approximation Eq. (1) with a dotted line, two terms approximation Eq. (4) with a dashed line, and three terms approximation Eq. (5) with a solid line. The mean FPT obtained from simulations equals 13.1, the median of distribution lies by 9.1. Note the logarithmic scale.

crossings for a stationary process, also known as the Rice frequency [28]. The general expression for n_0 reads

$$n_0 = \frac{1}{2\pi} \left(-\frac{r''_{xx}(0)}{r_{xx}(0)} \right)^{1/2} e^{-x_b^2/2r_{xx}(0)}. \quad (18)$$

In our case of a harmonic oscillator driven by white noise $n_0 = (\omega_0/2\pi) \exp(-\gamma x_b^2 \omega_0^2 / 2D)$. In the stationary regime the mean interval between two consecutive upcrossing T_R is given by the inverse of the Rice frequency $T_R = 1/n_0$. For the chosen parameter values $T_R = 8.06$.

The second approximation [gray line in Fig. 2(b)] reproduces almost exactly the first two peaks of FPT density. Then it becomes negative because in Eq. (4) trajectories performing two and more superfluous upcrossings are subtracted too many times. Moreover, the second approximation tends to minus infinity for $T \rightarrow \infty$. The third approximation reproduces well the three first peaks of $\mathcal{F}(T)$, and then diverges tending to plus infinity.

Note that the mean first passage time obtained numerically equals 14.6 for these parameter values, and the median of the distribution lies by 3.2. Thus the first three approximations reproduce the most part of the FPT probability density.

The behavior of $\mathcal{F}(T)$ for the harmonic oscillator with higher damping $\gamma=0.8$, stronger noise intensity $D=0.44$, and other parameters as in Fig. 2 is presented in Fig. 3. For these parameter values the relaxation time $t_{rel}=2.5$ is less than the period $T_p=6.86$. Therefore the FPT density is practically monomodal with a single maximum and a small shoulder separating it from the exponential tail. The numerically obtained $\mathcal{F}(T)$ is shown with gray crosses, the one term truncation with a dotted line, the two terms truncation with a dashed line, and the three terms truncation with a solid line. The truncation approximations reproduce again the most part of the distribution: the mean FPT equals 13.1 and the median lies by 9.1.

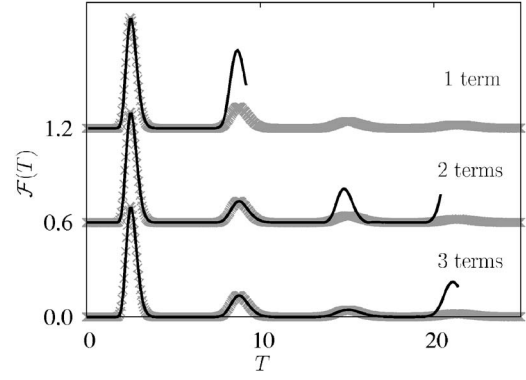


FIG. 4. The same as in Fig. 2, however, the truncations are correctly normalized by Eq. (19). Simulation results shown with gray crosses; the truncations with solid lines. The curves for normalized one, two, and three terms truncations are vertically shifted by 0.6 for the sake of clarity.

Thus the truncation approximations reproduce the FPT density on short times but are not normalized and diverge on large times. However, one can force the normalization in truncations as follows:

$$|\mathcal{F}_{trunc}(T)| \Theta \left(1 - \int_0^T |\mathcal{F}_{trunc}(t)| dt \right). \quad (19)$$

Here $\mathcal{F}_{trunc}(T)$ is a truncated series for the FPT density, it is given by Eqs. (1), (4), and (5) for one, two, and three terms truncations, respectively. $\Theta(t)$ is the Heaviside step function: the expression Eq. (19) turns to zero as soon as the integral over the absolute value of $\mathcal{F}_{trunc}(T)$ exceeds 1.

In Fig. 4 we show the FPT density for the same parameter values as in Fig. 2. Simulation results are shown with crosses, and approximations obtained from Eq. (19) with one, two, and three terms by solid lines. The probability distributed over the long exponential tail in the real FPT density is concentrated in the positive artifact posed on intermediate times in the normalized truncations. Hence the mean FPT computed from such approximations is always strongly underestimated.

The more terms are included, the more precise truncations become. However, one has to confine oneself to a few terms, since the calculation of higher order terms implies the computation of multiple integrals and is not more effective than simulations. Therefore the truncation approximations are good, when the most part of the FPT probability is concentrated in the first few peaks, i.e., when the barrier value is low or the noise is strong.

V. DECOUPLING APPROXIMATIONS

Decoupling approximations for Eq. (6) or Eq. (14) are based on approximate expressions of the higher order terms through the lower order ones, which may lead to a closed analytical form [32]. Thereby infinitely many approximate terms are included.

The simplest way to obtain such an approximation is to neglect all correlations between upcrossings. This means to

neglect all terms in Eq. (14) except for the first one, and leads to

$$S(T) = \int_0^T n_1(t) dt. \quad (20)$$

Equivalently, neglecting all correlations corresponds to the factorization of $n_{p+1}(T, t_p, \dots, t_1)$ into a product of one-point densities $n_1(T)n_1(t_p) \cdots n_1(t_1)$ in Eq. (6). Then the series, Eq. (6), sums up into $\mathcal{F}(T) \approx n_1(T) \exp(-\int_0^T n_1(t) dt)$, which is equivalent to Eqs. (13) and (20). This approximation will be referred to as the *Hertz approximation* since the form of $\mathcal{F}(T)$ resembles the Hertz distribution [33]. It is an approximation of first order, since it takes the first term of the series exactly, and all other terms are approximated through this first one.

The second order approximation should therefore account for the first and the second terms exactly and approximate all higher terms through these two. The general form of $\mathcal{F}(T)$ in terms of the cumulant functions Eq. (13) ensures the right normalization, irrespective of the way $S(T)$ is approximated. However, the simple truncation of the series Eq. (14) after the second term does not ensure the positive escape rate $S'(T)$.

The second order approximation guaranteeing $S'(T) > 0$ was proposed by Stratonovich in the context of peak duration [10]. The first and the second cumulant functions are taken exactly, and the higher ones are approximated by the combinations of these two:

$$g_p(t_p, \dots, t_1) \approx (-1)^{p-1} (p-1)! n_1(t_p) \cdots n_1(t_1) \times \{R(t_1, t_2) R(t_1, t_3) \cdots R(t_1, t_p)\}_s. \quad (21)$$

Here $\{\cdots\}_s$ is again the operation of symmetrization. $R(t_i, t_j)$ is the correlation coefficient of upcrossings

$$R(t_i, t_j) = 1 - \frac{n_2(t_i, t_j)}{n_1(t_i) n_1(t_j)}. \quad (22)$$

Note that $R(t_1, t_1) = 1$ and $R(t_i, t_j) \rightarrow 0$ for large values of $|t_i - t_j|$.

The approximation of the cumulant functions in the form Eq. (21) can be motivated by the following argument. Consider Eq. (10) with $r=1$. Recall that the joint densities of upcrossings vanish for coinciding arguments: $n_p(t_1, \dots, t_1) = 0$. Thus it follows from Eq. (10):

$$\ln[1 + n_1(t_1) z_1] = \sum_{p=1}^{\infty} \frac{1}{p!} g_p(t_1, \dots, t_1) z_1^p.$$

The above expression should hold for arbitrary z_1 . Therefore expanding the logarithm in series and equating the coefficients by the same powers of z_1 on both sides, one obtains the identity

$$g_p(t_1, \dots, t_1) = (-1)^{p-1} (p-1)! n_1^p(t_1). \quad (23)$$

Equation (23) is exact for all coinciding arguments. Equation (21) gives a correction to it, when the arguments differ.

Substitution of Eq. (21) into Eq. (14) delivers then the

Stratonovich approximation for $\mathcal{F}(T)$ in the form Eq. (13), now with $S(T)$ being

$$S(T) = - \int_0^T n_1(t) \frac{\ln \left[1 - \int_0^T R(t, t') n_1(t') dt' \right]}{\int_0^T R(t, t') n_1(t') dt'} dt. \quad (24)$$

Let us now discuss the domains of applicability for these approximations. The Hertz approximation Eq. (20) holds if all correlations decay considerably within the typical time interval between upcrossings T_R . The decay of correlations is described by the relaxation time $t_{rel} = 2/\gamma$ of the process. Therefore the Hertz approximation holds for $t_{rel} \ll T_R$.

The Stratonovich approximation is applicable when the argument of the logarithm in Eq. (24) is positive, $1 - \int_0^T [n_1(t') - n_1(t)^{-1} n_2(t', t)] dt' > 0$. Using the fact that $n_2(t', t)/n_1(t)$ tends to $n_1(t')$ for $|t-t'| > t_{rel}$ and tends to zero for $|t-t'| \rightarrow 0$ we get as a rough estimate for the validity region of Eq. (24) $t_{rel} < T_R$.

Let us now turn to the results for the harmonic oscillator Eq. (15) with white noise driving. In Figs. 5 and 6 the FPT probability density obtained from simulations is depicted with a gray line, the Hertz approximation Eq. (20) with a black dashed line, and the Stratonovich approximation Eq. (24) with a black solid line.

In Fig. 5(a) the parameters are chosen to be $\gamma=0.8$, $D=0.1$, corresponding to moderate friction and moderate noise intensity. For given parameter values $t_{rel}=2.5$ and $T_R=343$, so that $t_{rel} \ll T_R$, both Hertz and Stratonovich approximations hold and reproduce well the FPT density in the whole time domain.

In the case of moderate friction and stronger noise the upcrossings become more frequent and T_R decreases. The FPT changes its form to practically monomodal. An example is given in Fig. 5(b) with $\gamma=0.8$, $D=0.44$ which correspond to $t_{rel}=2.5$ and $T_R=15.6$. The Stratonovich approximation complies very well with simulations, while the Hertz approximation fails to reproduce the details of the distribution: It underestimates $\mathcal{F}(T)$ on short times, and shows slower exponential decay in the tail than the one observed in simulations (see the inset).

Finally, for small friction and weak noise the upcrossings are rare, but the relaxation time is large. The FPT probability density exhibits multiple decaying peaks. In Fig. 5(c) $\gamma=0.08$, $D=0.01$ corresponding to $t_{rel}=25$, $T_R=343$. Again, the Stratonovich approximation performs well, while the Hertz approximation underestimates the first peak, overestimates all further peaks, and decays in the tail faster than the simulated FPT density.

For the large T , $\mathcal{F}(T)$ decays exponentially, $\mathcal{F}(T) \propto \exp(-\kappa T)$. The decrement of this decay is obtained from the long time asymptotic: $\kappa T = \lim_{T \rightarrow \infty} S(T)$. Thus in the Hertz approximation Eq. (20) one gets $\kappa_H = \lim_{T \rightarrow \infty} (1/T) \int_0^T n_1(t) dt = n_0 T / T = n_0$. The behavior in the Stratonovich approximation Eq. (24) is determined by $\lim_{t, t' \rightarrow \infty} \int_0^T R(t, t') n_1(t') dt' \approx n_0 \tau_{cor}$ with τ_{cor} given by $\tau_{cor} = \lim_{t \rightarrow \infty} \int_0^{\infty} R(t, t') dt'$. Note that τ_{cor} is not necessarily positive because of the oscillating

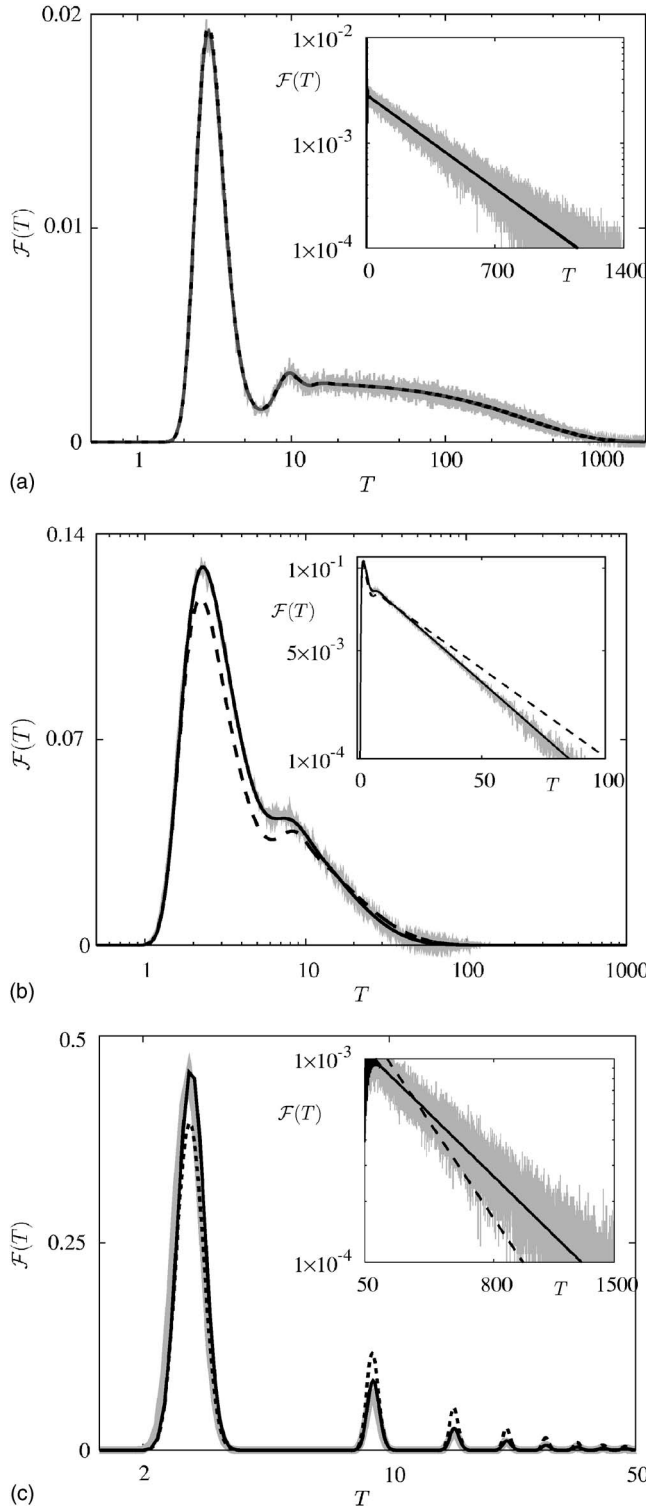


FIG. 5. FPT probability density for harmonic oscillator driven by Gaussian white noise. Simulation results are shown with a gray line, Hertz approximation with a black dashed line, and Stratonovich approximation with a black solid line. Note the logarithmic scale in T . The insets show the same curves on the logarithmic scale in $\mathcal{F}(T)$. The parameters are $\omega_0=1$, $x_0=-1$, $v_0=0$, $x_b=1$, (a) $\gamma=0.8$, $D=0.1$, $t_{rel}=2.5$, $T_R=343$, (b) $\gamma=0.8$, $D=0.44$, $t_{rel}=2.5$, $T_R=15.6$, and (c) $\gamma=0.08$, $D=0.01$, $t_{rel}=25$, $T_R=343$.

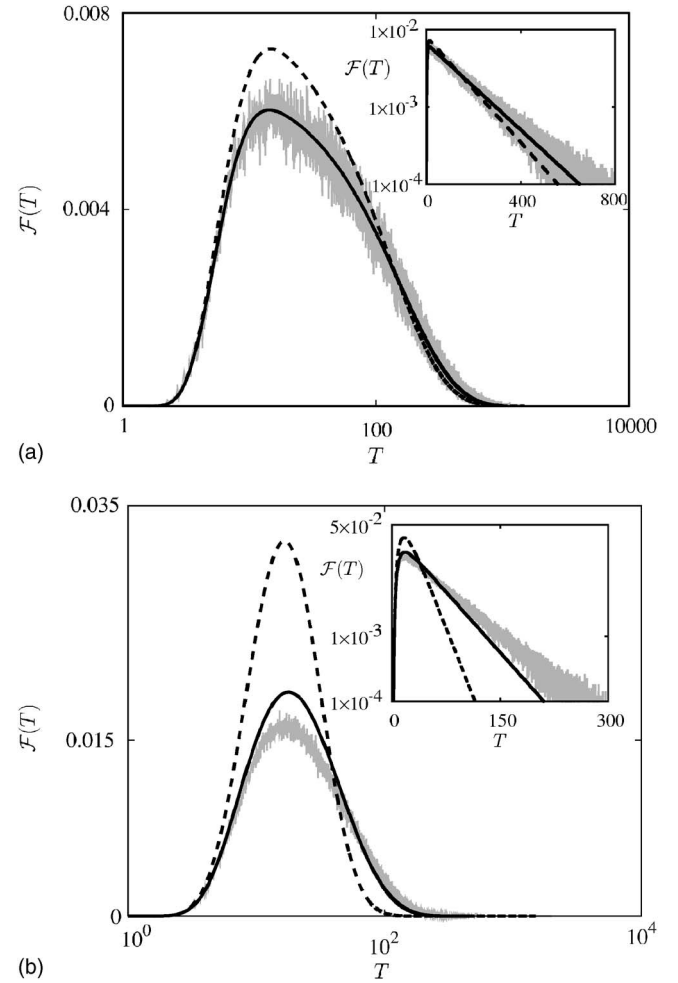


FIG. 6. Same as in Fig. 5, however, for the case of stronger friction. The parameters are (a) $\gamma=3.0$, $D=0.5$, $\omega_0/\gamma=0.33$, and (b) $\gamma=10.0$, $D=5.5$, $\omega_0/\gamma=0.1$ and other parameters as in Fig. 5.

correlation coefficient. Inserting this expression into Eq. (24) and expanding the logarithm up to the second term we get $\kappa_S = n_0(1 + \frac{1}{2}n_0\tau_{cor})$ providing the second order correction to κ_H . The value of τ_{cor} for the parameter set as in Fig. 5(a) is $\tau_{cor}=-2.4$, for parameters as in Fig. 5(b) $\tau_{cor}=5.09$, and for parameters as in Fig. 5(c) $\tau_{cor}=-431.99$. The long time asymptotic obtained with these τ_{cor} values reproduce fairly well the decay patterns found numerically.

In the overdamped regime ($\gamma > 2\omega_0$) the condition $t_{rel} < T_R$ is always fulfilled. Nevertheless the validity region of our approximations is limited. With increasing friction the process $x(t)$ approaches the Markovian one (it is Markovian in the overdamped limit $\omega_0/\gamma \ll 1$). For such processes the pattern of upcrossings is not homogeneous, but shows rather well separated clusters of upcrossings [10]. Essentially in the Markovian limit the property that upcrossings form a system of *nonapproaching* random points is violated. The upcrossings within a single cluster are not independent even if their mean density n_0 is low, so that the quality of approximations decreases. This fact is illustrated in Fig. 6. In the overdamped regime the correlation functions decay monotonously, and the FPT densities are always monomodal. The parameters in Fig. 6(a) are $\gamma=3.0$, $D=0.5$, so that

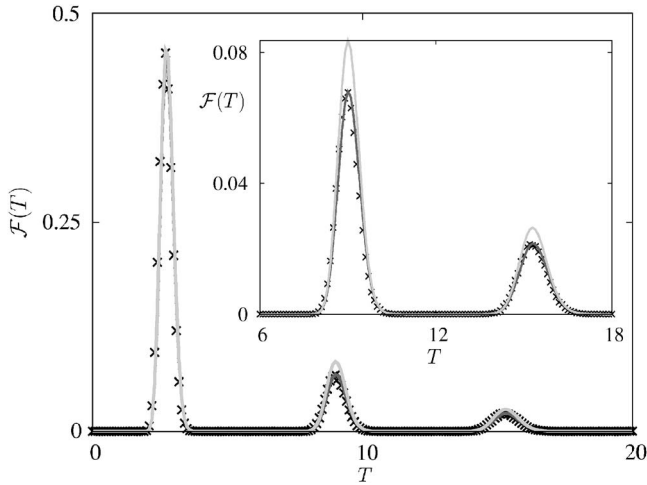


FIG. 7. FPT density for harmonic oscillator driven by white Gaussian noise, $\omega_0=1$, $\gamma=0.08$, $D=0.01$, $x_0=-1$, $v_0=0$, and $x_b=1$. Simulation results are shown with crosses, the three terms approximation with a black line, and the Stratonovich approximation with a gray line. The inset shows the magnification of a part of the curve.

$\omega_0/\gamma=0.33$. Equations (13) and (24) continue to give a good approximation for $\mathcal{F}(T)$, while the Hertz approximation becomes inaccurate. Further increase in friction, for example, $\gamma=10.0$, $D=5.5$ as in Fig. 6(b) corresponding to $\omega_0/\gamma=0.1$, makes the process approach the Markovian limit. The Stratonovich approximation starts to be inaccurate, and the Hertz approximation fails.

VI. TRUNCATION VERSUS DECOUPLING APPROXIMATIONS

In the two previous sections we have seen that truncation approximations reproduce the FPT density on short time scales. In contrast, the decoupling approximations reproduce FPT densities in the whole time domain and possess the right normalization. At first glance, it may seem that the decoupling approximations excel the direct truncations and should be preferably used in applications. However, it depends on the problem one has to solve, and sometimes the truncations turn out to be useful.

One such situation was already mentioned. If the noise intensity is high or the barrier value is low, then the upcrossings occur frequently, and the decoupling approximations cannot be applied. For example, for parameter values as in Fig. 2, the relaxation time is $t_{rel}=200$, and the mean interval between upcrossings $T_R=8.07$. Thus $t_{rel}>T_R$, and both Hertz and Stratonovich approximations fail. Nevertheless, the most part of the FPT density is concentrated in the first few peaks in this case, and is well reproduced by the truncation approximations, as shown in Figs. 2 and 4.

One can also be interested in a very accurate approximation for the FPT density on short times. The truncations deliver better results on short times than the decoupling approximations. For example, in Fig. 7 the simulation results are compared with the three terms truncation and the Stratonovich approximation for the same parameter values as in

Fig. 5(c). Both approximations reproduce very accurately the first peak in the FPT density. However, the three terms truncation is much more accurate in estimation of the second and third peaks (see the inset in Fig. 7).

This can be easily understood. The Stratonovich approximation takes $n_1(t_1)$ and $n_2(t_2, t_1)$ exactly, and approximates all higher order densities through these two. On times, when the first peak occurs, $n_2(t_2, t_1)$ is negligibly small. Then from Eqs. (21) and (22) we obtain $g_p(t_p, \dots, t_1) \approx (-1)^{p-1}(p-1)!n_1(t_p) \cdots n_1(t_1)$. Substitution of this expression into Eq. (10) then gives $n_p(t_p, \dots, t_1) \approx 0$ for $p > 1$. Thus on these times the Stratonovich approximation just coincides with the one term truncation, and so reproduces the first peak very accurately. On times, when the second peak in the FPT density occurs, $n_2(t_2, t_1)$ is significantly different from zero. Hence all approximated $n_p(t_p, \dots, t_1)$, $p > 2$ turn out to be nonvanishing as well, while the real values for these functions are negligibly small on these times. Thus the accuracy of the Stratonovich approximation decreases in the second peak. From analogous reasoning it becomes clear that the Hertz approximation is already inaccurate in estimation of the first peak.

VII. HARMONIC OSCILLATOR DRIVEN BY COLORED NOISE

Expressions Eq. (6) and Eqs. (13) and (24) can be used to obtain the FPT density for a random process $x(t)$ if the joint probability densities of x and its velocity v , Eq. (2), exist. Thus it is necessary that the process $x(t)$ is continuous and differentiable at any time, but there are no further restrictions on dimension and form of the system. The truncation and decoupling approximations deliver good results for the FPT density in their validity regions independently of the character of the noisy drive. In particular the case of correlated input signals (colored noise driving) is of importance in neuroscience. For example, synaptic filtering of the input spike train may lead to an exponentially correlated input signal.

Therefore we consider as another example a resonate-and-fire neuron Eq. (15) driven by the Ornstein-Uhlenbeck noise. The correlation time of the process is τ , the variance D/τ , and the correlation function $\langle \eta(t)\eta(t+t') \rangle = (D/\tau)\exp(-t'/\tau)$. In the limit $\tau \rightarrow 0$ the process tends to the white noise of intensity $2D$. The correlation functions $r_{xx}(t)$, $r_{xy}(t)$, $r_{yx}(t)$, $r_{xv}(t)=r'_{xx}(t)$, $r_{vv}(t)=-r''_{xx}(t)$, $r_{yv}(t)=r'_{yx}(t)$, $r_{vy}(t)=-r'_{xy}(t)$ can be obtained using Fourier transform as it was done for the white noise case in Sec. III.

Then $n_1(T)$ is again obtained analytically and has the form given by Eq. (17). Now $\mu_{ij}=\mu_{ji}$ are elements of the inverse correlation matrix $(\hat{C}_5)^{-1}$, q_i are components of vector $\vec{Q}=[x(T), v(T), x_0(0), v_0(0), \eta_0(0)]$. The factor α is defined in the same way as it was done in Sec. III.

For simplicity, we assumed sharp initial conditions for the noise variable, i.e., η is reset after every spike to a fixed value η_0 . The alternative assumption, that the neuron variables x, v are reset to their initial values once $x(t)$ reaches the threshold *without* resetting $\eta(t)$, might be more realistic [11]. In this case all probability densities should be averaged

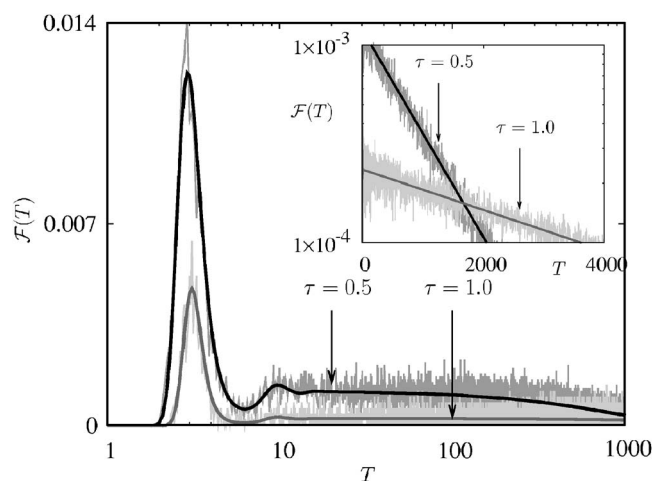


FIG. 8. Simulation results and the Hertz approximation for the FPT probability density for a harmonic oscillator driven by Ornstein-Uhlenbeck noise with correlation times $\tau=0.5$ (upper curves) and $\tau=1.0$ (lower curves) and other parameters as in Fig. 5(a). Note the logarithmic scale in T . The inset shows the same curves on the logarithmic scale in $\mathcal{F}(T)$.

with respect to the stationary density of noise values *upon firing*. However, as an example, we confine ourselves to consideration of sharp initial conditions for the noise: $P(\eta, t=0) = \delta(\eta - \eta_0)$.

In Fig. 8 we show simulated FPT probability density and the Hertz approximation for the harmonic oscillator driven by the Ornstein-Uhlenbeck noise. We choose two different values of the correlation time: $\tau=0.5$ and 1.0 . The reset value for the noise is $\eta_0=0$, and other parameters are as in Fig. 5(a). The noise intensity decreases with increasing τ , hence the mean FPT growth. For larger values of τ the height of the main peak decreases and the weight of the exponential tail growth, nevertheless $\mathcal{F}(T)$ preserves the bimodal structure. For given values of the correlation time $T_R=829.2$ and $T_R=4247.1$, respectively, that significantly exceeds t_{rel} . Thus in both cases the Hertz approximation is absolutely sufficient.

VIII. SUMMARY

Motivated by studies on the dynamics of resonant neurons, we consider the first passage time problem for systems with subthreshold oscillations and non-negligible relaxation

times after a reset. The joint densities of multiple upcrossings for such a process $x(t)$ can be obtained in the case of differentiable trajectories. The FPT density for $x(t)$ is expressed in terms of an infinite series of multiple integrals over all joint densities of upcrossings, or equivalently, in terms of the cumulant functions.

We consider two types of approximations for this infinite series. The truncation approximations include the first few terms of the series calculated exactly. They reproduce well the FPT density on short and intermediate times and can be used when the most part of the FPT probability is concentrated in the first few peaks, i.e., when the barrier value is low or the noise is strong.

The decoupling approximations can be derived for the case of weakly correlated upcrossings. The higher order cumulant functions are expressed through the lower order ones, and then infinitely many terms sum up to the closed expression for $\mathcal{F}(T)$. The Hertz approximation (the one neglecting all correlations between upcrossings) is absolutely sufficient for the case of moderate friction and moderate noise intensity. The Stratonovich approximation (approximating the higher order cumulant functions through the first and the second ones) performs even better and does not lose accuracy for high noise intensities or in the slightly overdamped regime.

We illustrate our results by the noise driven harmonic oscillator, with the threshold value at x_b and reset to sharp initial conditions, i.e., the resonate-and-fire model of a neuron. The validity regions of the approximations cover all different types of subthreshold dynamics. Thus the approximations reproduce all qualitatively different structures of the FPT densities: from monomodal through bimodal to multimodal densities with several decaying peaks. The approximations hold for systems of whatever dimension. We illustrate this by the harmonic oscillator driven by the Ornstein-Uhlenbeck noise.

Though we applied the theory to the harmonic oscillator (resonate-and-fire model), the linearity of the system is in general not required. The joint distributions of $x(t)$ and its velocity should exist, i.e., $x(t)$ should be differentiable in time. No further restrictions on the form and dimension of the system are implied.

ACKNOWLEDGMENT

We acknowledge financial support from the DFG through Graduierten Kolleg 268 and Sfb 555.

- [1] E. Schrödinger, *Phys. Z.* **16**, 289 (1915).
- [2] P. Hänggi, P. Talkner, and M. Borkovec, *Rev. Mod. Phys.* **62**, 251 (1990).
- [3] A. Longtin, A. Bulsara, and F. Moss, *Phys. Rev. Lett.* **67**, 656 (1991).
- [4] H. C. Tuckwell, *Introduction to Theoretical Neurobiology*, Vol. 2 (Cambridge University Press, Cambridge, UK, 1988).
- [5] S. Redner, *A Guide to First-Passage Processes* (Cambridge

- University Press, Cambridge, UK, 2001).
- [6] H. Risken, *The Fokker-Planck Equation* (Springer, Berlin, 1996).
- [7] N. G. van Kampen, *Stochastic Processes in Physics and Chemistry* (North-Holland, Amsterdam, 1992).
- [8] V. I. Tikhonov and M. A. Mironov, *Markovian Processes* (Sov. Radio, Moscow, 1977).
- [9] G. L. Gerstein and B. Mandelbrot, *Biophys. J.* **4**, 41 (1964).

- [10] R. L. Stratonovich, *Topics in the Theory of Random Noise*, Vol. 2 (Gordon and Breach, New York, 1967).
- [11] B. Lindner, Phys. Rev. E **69**, 022901 (2004).
- [12] D. Sigeiti and W. Horsthemke, J. Stat. Phys. **54**, 1217 (1989).
- [13] S. Liepelt, J. A. Freund, L. Schimansky-Geier, D. Russell, A. B. Neiman, and F. Moss, J. Theor. Biol. **237**, 30 (2005).
- [14] B. Lindner, J. García-Ojalvo, A. Neiman, and L. Schimansky-Geier, Phys. Rep. **392**, 321 (2004).
- [15] A. Fiasconaro, D. Valenti, and B. Spagnolo, Physica A **325**, 136 (2003).
- [16] A. Fiasconaro, B. Spagnolo, and S. Boccaletti, Phys. Rev. E **72**, 061110 (2005).
- [17] S. M. Soskin, V. I. Sheka, T. L. Linnik, and R. Mannella, Phys. Rev. Lett. **86**, 1665 (2001).
- [18] A. Mauro, F. Conti, F. Dodge, and R. Schor, J. Gen. Physiol. **55**, 497 (1970).
- [19] I. Erchova, G. Kreck, U. Heinemann, and A. V. M. Herz, J. Physiol. (London) **560**, 89 (2004).
- [20] N. Brunel, V. Hakim, and M. J. E. Richardson, Phys. Rev. E **67**, 051916 (2003).
- [21] D. T. W. Chik, Yuqing Wang, and Z. D. Wang, Phys. Rev. E **64**, 021913 (2001).
- [22] A. M. Lacasta, F. Sagues, and J. M. Sancho, Phys. Rev. E **66**, 045105(R) (2002).
- [23] T. Verechtchaguina, L. Schimansky-Geier, and I. M. Sokolov, Phys. Rev. E **70**, 031916 (2004).
- [24] E. I. Volkov, E. Ullner, A. A. Zaikin, and J. Kurths, Phys. Rev. E **68**, 026214 (2003).
- [25] V. A. Makarov, V. I. Nekorkin, and M. G. Velarde, Phys. Rev. Lett. **86**, 3431 (2001).
- [26] H. C. Tuckwell, BioSystems **80**, 25 (2005).
- [27] E. M. Izhikevich, Neural Networks **14**, 883 (2001).
- [28] S. O. Rice, Bell Syst. Tech. J. **24**, 51 (1945).
- [29] A. J. F. Siegert, Phys. Rev. **81**, 617 (1951).
- [30] Ya. A. Fomin, *Excursions Theory of Stochastic Processes* (Svyaz, Moscow, 1980).
- [31] C. Koch, *Biophysics of Computation* (Oxford University Press, Oxford, 1999).
- [32] T. Verechtchaguina, I. M. Sokolov, and L. Schimansky-Geier, Europhys. Lett. **73**, 691 (2006).
- [33] P. Hertz, Math. Ann. **67**, 387 (1909).